On aspects of the physical realizability of perfectly matched absorbers for electromagnetic waves

F. L. Teixeira

ElectroScience Laboratory and Department of Electrical Engineering, Ohio State University, Columbus, Ohio, USA

Received 13 November 2001; revised 23 April 2002; accepted 25 April 2002; published 6 February 2003.

[1] A discussion on the physical realizability of electromagnetic wave absorbers with perfectly matched impedances over arbitrary (i.e., doubly) curved, smooth surfaces is presented. The focus is on the analysis of the spectral characteristics (and their impact on the absorptive properties) of hypothetical material blueprints derived from the zero-reflection condition over such geometries. *INDEX TERMS:* 0619 Electromagnetics: Electromagnetic theory; 0689 Electromagnetics: Wave propagation (4275); 0699 Electromagnetics: General or miscellaneous; *KEYWORDS:* absorbers, perfectly matched layers

Citation: Teixeira, F. L., On aspects of the physical realizability of perfectly matched absorbers for electromagnetic waves, *Radio Sci.*, *38*(2), 8014, doi:10.1029/2001RS002559, 2003.

1. Introduction

1.1. Background

[2] Continual advances on microfabrication technology in recent years have made possible, particularly in two dimensions, the controlled design of novel material composites on scales down to tens of angstroms. For many cases in the microwave/millimeter-wave range, the observed electromagnetic behavior at such length scales and above is still essentially dominated by properties at a classical level, i.e., those governed by Maxwell's equations not augmented by any inherently quantum effects (or amenable to be described, for all practical purposes, by equivalent classical models). Motivated by such advances, entirely new classes of novel materials with superior electromagnetic properties in the microwave/millimeter-wave range have been recently proposed and/or demonstrated, including materials (ferroelectrics) with voltage tunable dielectric permittivities and (comparatively) small loss tangents at room temperature [*Sengupta and Klushens*, 1998], ultrahigh dielectric materials (e.g., carbon nanotubes) [*Garcia-Vidal et al.*, 1997; *Slepyan et al.*, 1998], photonic bandgap materials (PBGs, also-called electromagnetic bandgap materials, or EBGs) [*Yablonovitch*, 1993; *Sievenpiper et al.*, 1996; *Pendry et al.*, 1998; *Centeno and Felbacq*, 2000; *Kyriazidou et al.*, 2001], antiferroelectrics, (low-loss) magneto-dielectrics [*Walser et al.*, 1998; *Hansen and Burke*, 2000], left-handed materials (also-called double negative media or backward-wave media) [*Veselago*, 1967; *Smith et al.*, 2000; *Pendry*, 2000; *Smith et al.*, 2001; *Ziolkowski*, 2001; *Lindell et al.*, 2001; *Engheta*, 2001; *Tretyakov*, 2001], and low-k dielectrics [*Shieh et al.*, 1998; *Venugopal et al.*, 2000].

[3] One particular area in which microfabrication technology can have a definitive impact is on the design of wideband electromagnetic wave absorbers. A number of applications such as stealth technologies for radar cross-section (RCS) reduction and control, critically depend on the performance of antireflection composites [*Rozanov*, 2000]. Traditional designs of electromagnetic absorbers described in the open literature include Salisbury/Dallenbach screens and Jaumann absorbers [*Chambers and Ford*, 2000; *Fante and McCormack*, 1988], as well as ferrite-based absorbers [*Amin and James*, 1981]. The main limitations of classical designs are narrowband performance and their dependence on geometric properties of the coated surface. For instance, designs for planar surfaces show a degradation of the antireflection properties when placed over realistic curved surfaces, requiring extensive empirical corrections [*Hashimoto and Mizokami*, 1991]. In the last decade, there has been much interest in the possible use of chiral materials [*Jaggard and Engheta*, 1989; *Jaggard et al.*, 1990; *Bohren et al.*, 1992], and synthetic (bi)anisotropic materials with elementary (small) embedded scatterers of complex shape (helixes, omega shaped particles, etc.) [*Brewitt-Taylor*, 1994; *Norgren*, 1998; *Tretyakov*, 1998; *Simovski et al.*, 2000]. This allows, in principle, greater flexibility in the design of electromagnetic wave absorbers through the addition of extra degrees of

0048-6604/03/2001RS002559$11.00

freedom on the constitutive parameters, e.g., magnetoelectric effects.

1.2. PML Absorbers: Planar Case

[4] Around 1994, the concept of a perfect matched layer (PML) absorber was introduced in computational electromagnetics [*Berenger*, 1994]. The PML corresponds to a reflectionless absorption layer (for all frequencies and incidence angles) developed as an absorbing boundary condition (ABC) for computational purposes [*Berenger*, 1994; *Katz et al.*, 1994; *Chew and Weedon*, 1994; *Liu and He*, 1998]. Initially, such concept relied upon the introduction of matched artificial electric and magnetic conductivities and a splitting of the electromagnetic fields into subcomponents. Because of this, the resulting fields inside the PML layer were rendered nonphysical (non-Maxwellian). This was not of major relevance for the intended computational purposes per se, but it ruled out any physical interpretation for the reflectionless mechanism. Shortly thereafter, however, the PML concept has found an interesting dual formulation (Maxwellian PML) with a clear physical interpretation whereby the PML corresponds to particular frequency dependent material tensors (blueprints) $\bar{\bar{\epsilon}}$ and $\bar{\bar{\mu}}$ [*Sacks et al.*, 1995; *Gedney*, 1996; *Ziolkowski*, 1997a, 1997b]. These tensors are material blueprints which exhibit large and matched imaginary parts for the responsible absorption mechanism.

[5] Because of the complex characteristics of the PML tensors, their actual physical realizability is (as expected) not a trivial matter. Nevertheless, physically realizable absorber concepts have been proposed to mimic the perfectly matched absorber behavior over a broad range of frequencies. For instance, a broad bandwidth absorbing material, based on the planar Maxwellian PML and hence potentially realizable with a proper engineering of materials, was introduced by *Ziolkowski* [1997a] and further studied by *Ziolkowski* [1997b]. This proposal is based upon a generalization of the Lorentz model for the polarization and magnetization fields that includes an extra time derivative of the driving fields. Moreover, it was then shown that this potentially realizable medium is both causal and passively absorbing. Another interesting proposal of a PML-like material is based on the use of uniaxial omega composites with higher order spatial dispersion effects [*Tretyakov*, 1998].

1.3. Curved PMLs

[6] The PML was originally derived in Cartesian coordinates (planar PML). However, the effectiveness of a planar PML is greatly reduced when applied to curved surfaces of electrically small radius of curvature. The PML concept was later extended to curvilinear coordinates [*Chew et al.*, 1997; *Maloney et al.*, 1997; *Teixeira and Chew*, 1997a; *Collino and Monk*, 1998; *He and Liu*, 1999; *Hwang and Jin*, 1999]. Although the first such extensions have dealt with non-Maxwellian formulations only, it was later shown that Maxwellian PMLs could also be obtained in curvilinear geometries [*Teixeira and Chew*, 1998]. Such Maxwellian PMLs correspond to anisotropic material tensors with inhomogeneous properties depending on the local geometry (principal curvatures) of the termination (coated) surface. From the existence of such extensions, the question naturally emerges whether or not they could provide blueprints for physically realizable absorbers over curved surfaces, similarly to the planar PML case.

[7] For classification purposes, we may divide the study of the physical realizability of these such materials into three basic levels. The first level, denoted here *blueprint level*, amounts to investigating whether basic electromagnetic properties (i.e., causality, passivity) of the hypothetical material blueprints (frequency domain constitutive tensors) derived from the zero reflection conditions are satisfied [*Ziolkowski*, 1997b; *Norgren and He*, 1997]. The second level amounts to the search of time domain polarization models capable of approximating the desired response of the first level blueprints (ideal PML) at a given range of frequencies. At this second level, some compromise needs to be made on the frequency range under which such materials are expected to approximate the ideal PML behavior [*Ziolkowski*, 1997a; *Ziolkowski and Auzanneau*, 1997]. The third level consists on the investigation of specific material models (e.g., particulate composites with resonant, complex elementary scatterers) capable of furnishing the polarization responses derived at the second level [*Auzanneau and Ziolkowski*, 1998a, 1998b; *Tretyakov*, 1998, 2000]. Because of microfabrication constraints, additional compromises on the intended material performance are also present at this third level. (An additional level of analysis, apart from physical realizability studies but equally important for practical purposes, is related to the physical *feasibility* of such absorbers. This essentially amounts to the study of the structural (mechanical) and thermal conditions of any (physical level) proposed model and specific manufacturing constraints (e.g., thickness, density). A detailed numerical investigation at this level requires a multiphysics simulation approach.)

[8] As mentioned, for the planar PML, studies on the physical realizability of *planar* PML absorbers have been carried out at the different levels [*Ziolkowski*, 1997a; *Tretyakov*, 1998]. In this paper, we shall focus on the physical realizability of curved PML absorbers at the blueprint level.

2. Analysis

2.1. Curved PML Blueprints

[9] PML blueprints can be derived systematically for general geometries through a two step process. In the first step, a complexification of the metric of space is employed to map ordinary solutions of Maxwell's equations continuously into non-Maxwellian fields which exhibit a modified behavior (e.g., exponential decay) inside the PML [*Teixeira and Chew*, 1999a]. This complexification can be carried out by an analytic continuation of the spatial coordinates [*Teixeira and Chew*, 1998]. In the second step, another field mapping is employed. This second mapping transforms the non-Maxwellian (analytic continued) fields into a third set of fields, which are Maxwellian [*Teixeira and Chew*, 1999a]. This latter map explores the metric invariance of Maxwell's equations (in the sense of *Deschamps* [1981], *Teixeira and Chew* [1999b], and *Bossavit* [2001]), to recast the complexification of the metric as a change on the constitutive parameters. The end result is a set of Maxwell's equations in anisotropic media, where both the permeability and permittivity tensors are frequency dispersive and depend on the local metric coefficients of the PML surface (or, equivalently, the local radii of curvature of the PML).

[10] To describe these tensors, we attach a local orthogonal curvilinear coordinate system (ξ_1, ξ_2, ξ_3) to a point P on the PML surface, where ξ_1, ξ_2 are tangent coordinates to the surface and ξ_3 is the normal coordinate, such that $\xi_3 = 0$ represents the PML interface itself and $\xi_3 > 0$ represents points *inside* the PML. Using the convention $e^{-i\omega t}$, the PML blueprints for a doubly curved surface are written as

$$\bar{\bar{\epsilon}} = \epsilon \bar{\bar{\Lambda}} \tag{1a}$$

$$\bar{\bar{\mu}} = \mu \bar{\bar{\Lambda}} \tag{1b}$$

with the PML tensor [*Teixeira and Chew*, 1998]

$$\bar{\bar{\Lambda}} = \left(\frac{s h_1 \tilde{h}_2}{\tilde{h}_1 h_2}\right)\hat{t}_1\hat{t}_1 + \left(\frac{s \tilde{h}_1 h_2}{h_1 \tilde{h}_2}\right)\hat{t}_2\hat{t}_2 + \left(\frac{\tilde{h}_1 \tilde{h}_2}{s h_1 h_2}\right)\hat{n}\hat{n}, \tag{1c}$$

In the above, s is the so-called complex stretching variable [*Chew and Weedon*, 1994], which has a frequency dependence on the form $s(\omega, \xi_3) = a(\xi_3) + i\,\sigma(\xi_3)/\omega$, with $a(\xi_3) \geq 1$ and $\sigma(\xi_3) \geq 0$ in the PML ($\xi_3 > 0$) (other functional dependencies of s in terms of ω are possible as long as they lead to an absorptive behavior). The factors $\tilde{h}_i$ and h_i, $i = 1, 2$ are the stretched and nonstretched local metric coefficients, respectively, given by $h_i = r_i/r_{0i}$ and $\tilde{h} = \tilde{r}_i/r_{0i}$, $i = 1, 2$, and $h_3 = 1$, where $r_{0i}(\xi_1, \xi_2)$, $i = 1, 2$, are the local principal radii of curvature at the point $(\xi_1, \xi_2, 0)$. The radii of curvature are defined from the *outside* of the surface. Therefore, they are positive over concave surfaces and negative over convex surfaces. Moreover, $r_i = r_{0i} + \xi_3$ and $\tilde{r}_i = r_{0i} + \tilde{\xi}_3$ $i = 1, 2$, with

$$\tilde{\xi}_3 = \int_0^{\xi_3} s(\zeta)d\zeta = \int_0^{\xi_3} \left(a(\zeta) + i\frac{\sigma(\zeta)}{\omega}\right)d\zeta \equiv b(\xi_3) + i\frac{\Delta(\xi_3)}{\omega}. \tag{2}$$

being the analytic continuation of the coordinate ξ_3. The unit vectors $\hat{t}_i$, $i = 1, 2$, are tangential to S at P along the principal lines of curvature, and $\hat{n} = \hat{t}_1 \times \hat{t}_2$ is the unit vector normal to S at this point. In terms of the local coordinates ξ_1, ξ_2, ξ_3 of a local orthogonal system, we write $\hat{t}_i = (\partial\mathbf{r}/\partial\xi_i)/|\partial\mathbf{r}/\partial\xi_i|$, $i = 1, 2$, where $\mathbf{r}$ is the position vector, and analogously for $\hat{n}$. The imaginary part of the complex stretching variable s is responsible for the loss mechanism inside the PML region.

[11] The significance attached to equation (1) is that reflectionless absorption of incident waves on an curved surface can be obtained through by a hypothetical medium having properly chosen constitutive tensors. Strictly speaking, however, it is clear that the PML tensors given by equation (1) cannot represent the frequency behavior of real materials for all frequencies and, as a result, no physical significance can be attached to the absorber blueprint in equation (1) other than the (desired) constitutive behavior (objective function) to be *approximated* over some *finite*, preassigned bandwidth of interest. (For instance, in the limit $\omega \to \infty$ (in practice, this would correspond to the far ultraviolet for light element materials and X-ray frequencies for heavy element materials), a real material exhibits the following limiting approximate behavior for the permittivity (the fine structure is ignored for simplicity.) This has been the approach taken, for instance, in the work of *Ziolkowski* [1997a, 1997b] for physically realizable planar PMLs,

$$\epsilon_{ij}(\omega) \to \left(\epsilon_0 - \frac{\omega_p^2}{\omega^2}\epsilon_0 + i\frac{\omega_p^2\gamma}{\omega^3}\epsilon_0\right)\delta_{ij},$$

where $\omega_p^2 = Ne^2/m\epsilon_0$, N is the number of atoms per unit volume, e and m are the electron charge and mass, respectively, and γ is a damping constant related to the collision rate. This approximate dependence is not exhibited by equation (1). In terms of the permeability, slowly decaying μ_{ij} terms which decreases as $1/\omega$ may be present up to optical frequen-

cies for some anisotropic media such as ferromagnets. Also, some polarization modes related to the core electrons in the atoms may give rise to variations on the $\epsilon(\omega)$ behavior other than above even at X-ray frequencies, but this is not germane to the main discussion here.)

2.2. Inhomogeneous Properties and Frequency Behavior

[12] In the case of planar PMLs, $r_{0i} \to \infty$, $h_i \to 1$, and $\tilde{h}_i \to 1$, so that equation (1) reduces to the simpler form

$$\overline{\overline{\Lambda}} = s\left(\overline{\overline{I}} - \hat{n}\hat{n}\right) + \frac{1}{s}\hat{n}\hat{n} \tag{3}$$

[13] Meaningful microscopical time domain models can be obtained for equation (3) by using, for example, Lorentz models for the polarization $\overline{P}$ and magnetization $\overline{M}$ fields near the resonance (which implies, however, a narrowband performance if high absorption is desired), or, for more broadband behavior, through time-derivative Lorentz medium models for both $\overline{P}$ and $\overline{M}$ [*Ziolkowski*, 1997a].

[14] The more complicated nature of the curved PML blueprint $\overline{\overline{\Lambda}}$ given by equation (1), when compared to the planar PML given by equation (3) is a consequence of the presence of the metric factors $\tilde{h}_i/h_i$. The properties of the curved PML differ in two major ways from those of the planar PML:

1. The curved PML tensor consist of rational functions of ω involving higher order polynomials than the planar case. As a result, higher order time-derivatives will need to be present in equivalent polarization and magnetization time domain models.

2. The curved PML is, in general, an inhomogeneous medium in the transverse directions (ξ_1, ξ_2) because the metric factors in equation (1) depend on the local radii of curvature $r_{0i}(\xi_1, \xi_2)$, $i = 1, 2$.

[15] Both these facts lead to additional complexity for the necessary material engineering. A more fundamental aspect for the physical realizability, however, is the impact that the metric factors $\tilde{h}_i/h_i$ have on the *spectral* properties (when treating ω as a complex variable) of the PML blueprints. This is discussed next.

2.3. Spectral Properties; Limitations

[16] An important mathematical property to be observed by any constitutive parameter of a real passive material is the Kramers-Kronig (KK) relations [*Landau et al.*, 1984]. The KK relations are often assumed to be a necessary condition for a material response to satisfy the *primitive* causality conditions (i.e., an effect cannot precede its cause). In terms of the constitutive relations, this is equivalent to the requirement $\overline{\overline{\epsilon}}(t) = \overline{\overline{\mu}}(t) = 0$ for $t < 0$. However, the KK relations are indeed only a sufficient condition for primitive causality, as will be discussed later.

[17] The KK relations applied to the PML tensor in equation (1) read as

$$\Re e\left[\overline{\overline{\Lambda}}(\omega)\right] - \overline{\overline{\Lambda}}(\infty) = \mathcal{H}\left[\Im m\left[\overline{\overline{\Lambda}}(\omega')\right]\right] = \frac{1}{\pi} PV \int_{-\infty}^{+\infty} \frac{\Im m\left[\overline{\overline{\Lambda}}(\omega')\right]}{\omega' - \omega} d\omega' \tag{4a}$$

$$\Im m\left[\overline{\overline{\Lambda}}(\omega)\right] = -\frac{1}{\pi} PV \int_{-\infty}^{+\infty} \frac{\Re e\left[\overline{\overline{\Lambda}}(\omega')\right] - \overline{\overline{\Lambda}}(\infty)}{\omega' - \omega} d\omega' + \frac{\overline{\overline{\sigma}}}{\omega} \tag{4b}$$

for ω and ω' real and where $\overline{\overline{\Lambda}}(\infty) \equiv \lim_{\omega \to \infty} \overline{\overline{\Lambda}}(\omega)$ is a real constant. In the above, PV denotes the Cauchy principal value, $\mathcal{H}$ is a Hilbert transform, and $\overline{\overline{\sigma}} = -iRes[\overline{\overline{\Lambda}}(\omega)]_{\omega=0} = -i \lim_{\omega \to 0} \omega \overline{\overline{\Lambda}}(\omega)$. We call equation (4) *generalized KK relations* because they include an extra term in equation (4b) (residue contribution) due the pole at $\omega = 0$, originating from (static) conductive losses in the PML [*Teixeira and Chew*, 1999c].

[18] In the case of the PML blueprints for curved surfaces, there is a major asymmetry between the spectral properties of $\overline{\overline{\Lambda}}(\omega)$ according to the local radii of curvature. This asymmetry directly impacts the validity of the generalized KK relations for $\overline{\overline{\Lambda}}(\omega)$. In order to study it more carefully, we first introduce some definitions.

Definition 1. A *Concave or Planar* (CoP) surface point is such that $\kappa_{0i} \geq 0$ on it, for $i = 1, 2$ where $\kappa_{0i} = 1/r_{0i}$ are the local curvatures.

Definition 2. A *Nonplanar, Nonconcave* (NPNC) surface point is such that $\kappa_{01} < 0$ or $\kappa_{02} < 0$ on it.

[19] We have the following result for CoP surfaces.

Proposition 1. *The PML tensor $\overline{\overline{\Lambda}}(\omega)$ at a CoP surface point satisfies the generalized KK relations*.

Proof. Equation (4) are a consequence of the application of the Cauchy's theorem to the function $(\overline{\overline{\Lambda}}(\omega') - \overline{\overline{\Lambda}}(\infty))/(\omega' - \omega)$ on the upper half of the complex ω plane (UHP), under the hypothesis that $\overline{\overline{\Lambda}}(\omega')$ is analytic (holomorphic) there [*Landau and Lifshitz*, 1980]. Therefore, the proof just amounts to showing that $\overline{\overline{\Lambda}}(\omega)$ is analytic on UHP.

[20] In a concave or planar surface point $P = (\xi_1, \xi_2, \xi_3)$, we rewrite equation (1c) explicitly as

$$\overline{\overline{\Lambda}} = \Lambda_{11}\hat{t}_1\hat{t}_1 + \Lambda_{22}\hat{t}_2\hat{t}_2 + \Lambda_{33}\hat{n}\hat{n}, \tag{5}$$

with

$$\Lambda_{11} = \frac{sh_1\tilde{h}_2}{\tilde{h}_1 h_2} = \frac{(a(\xi_3) + i\sigma(\xi_3)/\omega)(r_{01}(\xi_1,\xi_2) + \xi_3)(r_{02}(\xi_1,\xi_2) + b(\xi_3) + i\Delta(\xi_3)/\omega)}{(r_{02}(\xi_1,\xi_2) + \xi_3)(r_{01}(\xi_1,\xi_2) + b(\xi_3) + i\Delta(\xi_3)/\omega)} \tag{6a}$$

$$\Lambda_{22} = \frac{sh_2\tilde{h}_1}{\tilde{h}_2 h_1} = \frac{(a(\xi_3) + i\sigma(\xi_3)/\omega)(r_{02}(\xi_1,\xi_2) + \xi_3)(r_{01}(\xi_1,\xi_2) + b(\xi_3) + i\Delta(\xi_3)/\omega)}{(r_{01}(\xi_1,\xi_2) + \xi_3)(r_{02}(\xi_1,\xi_2) + b(\xi_3) + i\Delta(\xi_3)/\omega)} \tag{6b}$$

$$\Lambda_{33} = \frac{\tilde{h}_1\tilde{h}_2}{sh_1 h_2} = \frac{(r_{01}(\xi_1,\xi_2) + b(\xi_3) + i\Delta(\xi_3)/\omega)(r_{02}(\xi_1,\xi_2) + b(\xi_3) + i\Delta(\xi_3)/\omega)}{(a(\xi_3) + i\sigma(\xi_3)/\omega)(r_{02}(\xi_1,\xi_2) + \xi_3)(r_{01}(\xi_1,\xi_2) + \xi_3)} \tag{6c}$$

From the above, the singularities of $\overline{\overline{\Lambda}}(\omega)$ are found to be simple poles located at

$$\omega_0 = 0 \tag{7a}$$

$$\omega_1 = -i\frac{\Delta(\xi_3)}{r_{01}(\xi_1,\xi_2) + b(\xi_3)} \tag{7b}$$

$$\omega_2 = -i\frac{\Delta(\xi_3)}{r_{02}(\xi_1,\xi_2) + b(\xi_3)} \tag{7c}$$

$$\omega_4 = -i\frac{\sigma(\xi_3)}{a(\xi_3)} \tag{7d}$$

For $\xi_3 \geq 0$, we have $a(\xi_3) \geq 1$ and $\sigma(\xi_3) \geq 0$ and therefore, from equation (2), $b(\xi_3) \geq \xi_3 \geq 0$, and $\Delta(\xi_3) \geq 0$. For a concave surface $r_{01}(\xi_1, \xi_2) > 0$ and $r_{02}(\xi_1, \xi_2) > 0$ by definition and hence, from equations (7a) and (7b), both ω_1, ω_2, and ω_3 are located on the lower half of the complex ω plane (LHP). For a planar surface, $\Lambda_{11} = \Lambda_{22} = s$ and $\Lambda_{33} = 1/s$ and hence the only poles are $\omega_0 = 0$ and $\omega_4 = -i\sigma(\xi_3)/a(\xi_3)$. Therefore, for a planar or concave surface no singularities for $\overline{\overline{\Lambda}}(\omega)$ are present on the UHP, and $\overline{\overline{\Lambda}}(\omega)$ is analytic there. ♢

[21] A different conclusion is obtained for NPNC surfaces, as described by the next proposition.

Proposition 2. *The PML tensor $\overline{\overline{\Lambda}}(\omega)$ at a NPNC surface point for which $\kappa_{01} \neq \kappa_{02}$ violates the generalized KK relations.*

Proof. In this case, the PML tensor again writes as equations (5)–(6), and we still have, for $\xi_3 \geq 0$, that $b(\xi_3) \geq \xi_3 \geq 0$ and $\Delta(\xi_3) \geq 0$. However, by definition $r_{01}(\xi_1, \xi_2) < 0$ or $r_{02}(\xi_1, \xi_2) < 0$ for a NPNC surface point and therefore at least one of the poles ω_1, ω_2 will be located on the UHP. As a result, $\overline{\overline{\Lambda}}(\omega)$ is not analytic on the UHP. If in the UHP, we denote these poles λ_1 and λ_2 (the latter may not exist). Given a $\overline{\overline{\Lambda}}(\omega')$ tensor with simple poles on the UHP at $\omega' = \lambda_k$, $k = \overline{1,N}$, the application of Cauchy's theorem to the associated tensor $\overline{\overline{F}}(\omega, \omega') = (\overline{\overline{\Lambda}}(\omega') - \overline{\overline{\Lambda}}(\infty))/(\omega' - \omega)$ on the UHP of ω' gives

$$PV\int_{-\infty}^{+\infty} \overline{\overline{F}}(\omega,\omega')d\omega' - \pi i Res\left[\overline{\overline{F}}(\omega,\omega')\right]_{\omega'=0} - \pi i Res\left[\overline{\overline{F}}(\omega,\omega')\right]_{\omega'=\omega} + \int_{C_\infty} \overline{\overline{F}}(\omega,\omega')d\omega' = 2\pi i\sum_{k=1}^{N} Res\left[\overline{\overline{F}}(\omega,\omega')\right]_{\omega'=\lambda_k} \tag{8}$$

where ω is real, and the right hand side of equation (8) is a sum over all the residues of $\overline{\overline{F}}(\omega, \omega')$ on the UHP of ω', $N = 1$ or $N = 2$ for $\overline{\overline{\Lambda}}(\omega)$ as in equations (5)–(6). The last integral on the left hand side of equation (8) is carried out at a semicircle at infinity, C_∞. Since $\lim_{\omega'\to\infty} \overline{\overline{F}}(\omega, \omega') = 0$, the integration over C_∞ vanishes. The two residue contributions on the left hand side of equation (8) are due to small indentations above the singularities of $\overline{\overline{F}}(\omega, \omega')$ on the real axis at $\omega' = 0$ and $\omega' = \omega$.

[22] By writing

$$\overline{\overline{\Lambda}}(\omega) = \overline{\overline{\Lambda}}_0(\omega) + i\frac{\overline{\overline{\sigma}}}{\omega}$$

where $\overline{\overline{\Lambda}}_0(\omega)$ is analytic at $\omega = 0$, we have

$$\overline{\overline{F}}(\omega,\omega') = \frac{\overline{\overline{\Lambda}}_0(\omega') - \overline{\overline{\Lambda}}(\infty)}{\omega' - \omega} + i\frac{\overline{\overline{\sigma}}}{\omega'(\omega' - \omega)}$$

and therefore

$$Res\left[\overline{\overline{F}}(\omega,\omega')\right]_{\omega'=0} = -i\frac{\overline{\overline{\sigma}}}{\omega}$$

$$Res\left[\overline{\overline{F}}(\omega,\omega')\right]_{\omega'=\omega} = \overline{\overline{\Lambda}}_0(\omega) - \overline{\overline{\Lambda}}(\infty) + i\frac{\overline{\overline{\sigma}}}{\omega} = \overline{\overline{\Lambda}}(\omega) - \overline{\overline{\Lambda}}(\infty)$$

$$Res\left[\overline{\overline{F}}(\omega,\omega')\right]_{\omega'=\lambda_k} = -\frac{Res\left[\overline{\overline{\Lambda}}(\omega')\right]_{\omega'=\lambda_k}}{\omega - \lambda_k}$$

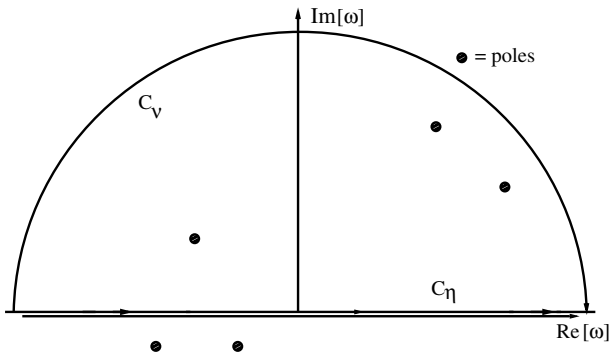

Figure 1. Noncausal Fourier inversion contour C_η for $\Lambda(\omega)$ with singularities in the upper-half of the complex ω plane.

As a result, equation (8) becomes

$$PV\int_{-\infty}^{+\infty}\frac{\overline{\overline{\Lambda}}(\omega')-\overline{\overline{\Lambda}}(\infty)}{\omega'-\omega}d\omega'-\pi\frac{\overline{\overline{\sigma}}}{\omega}-\pi i\left(\overline{\overline{\Lambda}}(\omega)-\overline{\overline{\Lambda}}(\infty)\right)$$

$$=-2\pi i\sum_{k=1}^{N}\frac{Res\left[\overline{\overline{\Lambda}}(\omega')\right]_{\omega'=\lambda_k}}{\omega-\lambda_k} \tag{9}$$

Separating the real and imaginary part of the above we have

$$\Re e\left[\overline{\overline{\Lambda}}(\omega)\right]-\overline{\overline{\Lambda}}(\infty)=\frac{1}{\pi}PV\int_{-\infty}^{+\infty}\frac{\Im m\left[\overline{\overline{\Lambda}}(\omega')\right]}{\omega'-\omega}d\omega'$$

$$+2\sum_{k=1}^{N}Res\left[\overline{\overline{\Lambda}}(\omega')\right]_{\omega'=\lambda_k}\Re e\left[\frac{1}{\omega-\lambda_k}\right] \tag{10a}$$

$$\Im m\left[\overline{\overline{\Lambda}}(\omega)\right]=-\frac{1}{\pi}PV\int_{-\infty}^{+\infty}\frac{\Re e\left[\overline{\overline{\Lambda}}(\omega')\right]-\overline{\overline{\Lambda}}(\infty)}{\omega'-\omega}d\omega'$$

$$+\frac{\overline{\overline{\sigma}}}{\omega}+2\sum_{k=1}^{N}Res\left[\overline{\overline{\Lambda}}(\omega')\right]_{\omega'=\lambda_k}\Im m\left[\frac{1}{\omega-\lambda_k}\right] \tag{10b}$$

where have used, from equations (6)–(7), that $Res\left[\overline{\overline{\Lambda}}(\omega')\right]_{\omega'=\lambda_k}$ are constant and purely real tensors. Equation (10) are the counterpart to the generalized KK relations at a NPNC surface point. Both the residues of $\Lambda_{11}(\omega')$ and $\Lambda_{22}(\omega')$ at $\omega' = \omega_1$ and $\omega' = \omega_2$, respectively, may contribute to $Res\left[\overline{\overline{\Lambda}}(\omega')\right]_{\omega'=\lambda_k}$.

[23] Furthermore, from equations (5)–(6) we have

$$Res[\Lambda_{11}(\omega')]_{\omega'=\omega_1}=(r_{02}-r_{01})\left(\frac{r_{01}+\xi_3}{r_{02}+\xi_3}\right)\cdot\left[a-\sigma\left(\frac{r_{01}+b}{\Delta}\right)\right] \tag{11a}$$

$$Res[\Lambda_{22}(\omega')]_{\omega'=\omega_2}=(r_{01}-r_{02})\left(\frac{r_{02}+\xi_3}{r_{01}+\xi_3}\right)\cdot\left[a-\sigma\left(\frac{r_{02}+b}{\Delta}\right)\right] \tag{11b}$$

where, from equation (2), a, b, σ and Δ are in general functions of position (ξ_3 coordinate). Therefore, unless we have $r_{01} = r_{02}$, the summation terms in the right-hand side of equation (10) are nonzero and equation (10) do not reduce to equation (4). $\diamondsuit$

2.4. Time Domain Response

[24] As mentioned before, violation of the KK relations for a function $\overline{\overline{\chi}}(\omega)$ does not necessarily render a corresponding time domain transform $\overline{\overline{\chi}}(t)$ noncausal. The actual behavior of $\overline{\overline{\chi}}(t)$ depends on the particular choice for the Fourier inversion contour used to invert $\overline{\overline{\chi}}(\omega)$. A noncausal $\overline{\overline{\chi}}(t)$ is obtained if an inverse Fourier contour along the real axis is used, as illustrated in Figure 1. On the other hand, a causal $\overline{\overline{\chi}}(t)$ is obtained using a contour C_γ taken above all singularities, as illustrated in Figure 2. In the latter case, the inverse Fourier transform

$$\overline{\overline{\chi}}(t)=\frac{1}{2\pi}\int_{C_\gamma}\overline{\overline{\chi}}(\omega)e^{-i\omega t}dw \tag{12}$$

can be closed, when $t < 0$, from the above by the semicircle at infinity $C_\nu \to C_\infty$ (Figure 2), which yields

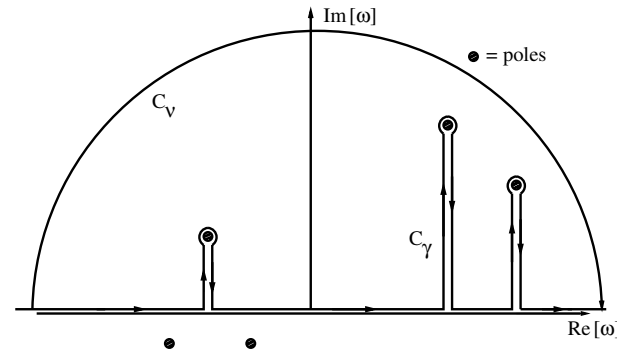

Figure 2. Causal Fourier inversion contour C_γ for $\Lambda(\omega)$ with singularities in the upper-half of the complex ω plane. No singularity is enclosed by $C_\gamma - C_\nu$.

$\overline{\overline{\chi}}(t) = 0$ after applying Jordan's lemma. For $t > 0$, on the other hand, the contour C_γ can be closed from below, and application of Cauchy's theorem and Jordan's lemma yields

$$\overline{\overline{\chi}}(t) = \frac{1}{2\pi}\sum_{k=1}^{N_1}\overline{\overline{A}}_k e^{-i\lambda_k t} + \frac{1}{2\pi}\sum_{k=1}^{N_2}\overline{\overline{B}}_k e^{-i\upsilon_k t} \qquad (13)$$

where we have assumed for simplicity [and according to equations (5)–(6)], a $\overline{\overline{\chi}}(\omega)$ tensor in equation (12) having simple poles $\omega = \lambda_k$, $k = 1, \ldots, N_1$ in the UHP ($\Im m[\lambda_k] > 0$) and single poles $\omega = \upsilon_k$, $k = 1, \ldots, N_2$ elsewhere ($\Im m[\upsilon_k] \leq 0$) as the only singularities. (The discussion remains essentially the same if multiple poles or branch point are present. In the first case, the summation should include terms of the form $\overline{\overline{p}}_k(t)e^{-i\lambda_k t}$ and/or $\overline{\overline{p}}_k(t)e^{-i\upsilon_k t}$, where $\overline{\overline{p}}_k(t)$ is an $(n-1)$-th order tensor polynomial and n is the multiplicity of the pole at $\omega = \lambda_k$ and/or $\omega = \upsilon_k$, respectively. In the second case, the summation should include terms of the form $\overline{\overline{f}}_k(t)e^{-i\beta_k t}$, where β_k is a branch point at $\omega = \beta_k$ and $\overline{\overline{f}}_k(t)$ depends on the difference of $\overline{\overline{\chi}}(\omega)$ along the two sides of the corresponding branch cut.) The summation at the left in equation (13) corresponds to the residue contributions from the UHP poles (UHP associated eigenmodes), while the summation at the right corresponds to the residue contributions from the poles elsewhere. Because $\Im m[\lambda_k] > 0$, any term in the summation at the left is an unbounded function *with exponential increase in time*.

[25] In the previous section, we have determined that the PML blueprint $\overline{\overline{\Lambda}}(\omega)$ at a NPNC surface point with $\kappa_{01} \neq \kappa_{02}$ has at least one pole in the UHP. Because of this, the expression for susceptibility-like kernel $\overline{\overline{\Lambda}}(t)$ reads as equation (13) with at least one term in the summation at the left. As a result, $\overline{\overline{\Lambda}}(t)$ is unbounded function and such PML corresponds to an hypothetical medium which have internal sources of energy, i.e., artificially injects energy into the field (spurious active behavior), and not to an absorber medium. We also note here that for the degenerate case of NPNC surface points with $\kappa_{01} = \kappa_{02}$, both residues in equation (11) are zero and hence the generalized KK relations are satisfied. Despite of that, a spurious active behavior is still present. In this case, this behavior is associated with the presence of *zeros* for $\overline{\overline{\Lambda}}(\omega)$ in the UHP [*Aki and Richards*, 1980; *Landau and Lifshitz*, 1980]. From equation (6c) with $r_{01} = r_{02} = r_0$, we write

$$\Lambda_{33}(\omega) = \frac{1/a}{\omega\left(\omega + i\frac{\sigma}{a}\right)}\left(\frac{r_0 + b}{r_0 + \xi_3}\right)^2\left(\omega + i\frac{\Delta}{r_0 + b}\right)^2 \qquad (14)$$

and we see that a double zero is present on the imaginary $\Im m[\omega]$ axis at the point $\omega = -i\sigma/(r_0 + b)$. In a NPNC surface $r_0 < 0$ and this double zero is on the UHP. Hence, a similar analysis to the previous section can be made for the reciprocal kernel $\overline{\overline{\Lambda}}^{-1}(\omega)$ with UHP singularities. (For simplicity, we have been focusing exclusively on the impact of the spectral properties of $\overline{\overline{\Lambda}}$ on the constitutive equations. From the vector wave equation

$$\nabla \times \overline{\overline{\mu}}^{-1} \cdot \nabla \times \overline{E} - \omega^2 \overline{\overline{\epsilon}} \cdot \overline{E} = 0$$

we arrive, in the case of a PML medium, at

$$\nabla \times \overline{\overline{\Lambda}}^{-1} \cdot \nabla \times \overline{E} - \omega^2 \mu\epsilon \overline{\overline{\Lambda}} \cdot \overline{E} = 0$$

which depends explicitly both on $\overline{\overline{\Lambda}}(\omega)$ *and its inverse*.) On the contrary, for a CoP surface point, neither poles nor zeros are present on the UHP.

[26] The spurious behavior of PML blueprints on NCNP surfaces discussed above has been observed in time domain numerical simulations employing such hypothetical media in curvilinear grids [*Teixeira and Chew*, 1999c; *Teixeira et al.*, 2001]. In these simulations, the behavior has manifested itself in terms of a strong dynamic instability established as soon as the incident wave impinges upon a NCNP PML region.

[27] It should be mentioned at this point that *approximate* PML blueprints can nevertheless still be obtained for NCNP geometries based on slight modifications from the exact PML blueprints. This could be done, for instance, by *enforcing* the poles and zeros in equation (6) to be on the LHP. Any such a posteriori modification would lead to blueprint absorbers suitable in principle for any geometries, but without reflectionless properties. In particular, enforcing $\Delta(\xi_3) = 0$ (planar PML) achieves this objective. Again, the performance of these blueprints depends on the local radii of curvature, with large radii ones exhibiting better performance (smaller reflections).

3. Conclusions

[28] We have discussed some theoretical aspects for the physical realizability of material blueprints for the reflectionless absorption of electromagnetic waves on general surface geometries.

[29] The results presented here have indicated that PML (i.e., reflectionless) absorber blueprints could not be established on all surface geometries. This is because the imposition of reflectionless conditions on some geometries (at NPNC surface points) is theoretically irreconcilable with absorptive effects. The resulting blueprints on such geometries exhibit a spurious active

behavior (internal sources of energy) which manifest as unbounded time domain susceptibilities.

[30] This conclusion has been established against the backdrop of PML blueprint models that reduce to the usual planar PML in the limit of infinite radii of curvature [i.e., $\overline{\overline{\epsilon}} = \epsilon\overline{\overline{\Lambda}}(\omega)$ and $\overline{\overline{\mu}} = \mu\overline{\overline{\Lambda}}(\omega)$, with $\overline{\overline{\Lambda}}$ given by equation (3)], which is an important condition to ensure compatibility in complex objects composed of both planar and curved surfaces. Consequently, this analysis does not rule out the existence of *dissimilar* reflectionless absorber blueprints for NCNP geometries (i.e., which do not reduce to the usual planar PML in the limit of infinite radii of curvature). Such possibility is currently under investigation.

[31] **Acknowledgments.** This work was presented in part at the 2001 URSI International Symposium on Electromagnetic Theory, Victoria, Canada, 13–17 May 2001.

References

Aki, K., and P. G. Richards, *Quantitative Seismology, Theory and Methods*, vol. 1, W. H. Freeman, New York, 1980.

Amin, M. B., and J. R. James, Techniques for utilization of hexagonal ferrites in radar absorbers, 1, Broadband planar coatings, *Radio Electron. Eng. (London)*, *51*, 209–218, 1981.

Auzanneau, F., and R. W. Ziolkowski, Microwave signal rectification using artificial composite materials composed of diode-loaded electrically small dipole antennas, *IEEE Trans. Microwave Theory Tech.*, *46*(11), 1628–1637, 1998a.

Auzanneau, F., and R. W. Ziolkowski, Theoretical study of synthetic bianisotropic materials, *J. Electromagn. Waves Appl.*, *12*, 353–370, 1998b.

Berenger, J. P., A perfectly matched layer for the absorption of electromagnetic waves, *J. Comput. Phys.*, *114*(2), 185–200, 1994.

Bohren, C. F., R. Luebbers, H. S. Langdon, and F. Hunsenberger, Microwave-absorbing chiral composites: Is chirality essential or accidental?, *Appl. Opt.*, *31*(30), 6403–6407, 1992.

Bossavit, A., 'Generalized finite differences' in computational electromagnetics, in *Geometric Methods for Computational Electromagnetics, Progress in Electromagnetics Research*, *PIER 32*, edited by F. L. Teixeira, pp. 45–64, EMW Publishing, Cambridge, Mass., 2001.

Brewitt-Taylor, C. R., Modeling of helix-loaded chiral radar-absorbing layers, in *Progress in Electromagnetics Research*, *PIER 9*, edited by J. A. Kong, pp. 288–310, Elsevier Sci., New York, 1994.

Centeno, E., and D. Felbacq, Light propagation control by finite-size effects in photonic crystals, *Phys. Lett. A*, *292*, 165–169, 2000.

Chambers, B., and K. L. Ford, Topology for tunable radar absorbers, *Electron. Lett.*, *36*(15), 1304–1306, 2000.

Chew, W. C., and W. Weedon, A 3D perfectly matched medium from modified Maxwell's equations with stretched coordinates, *Microwave Opt. Technol. Lett.*, *7*(13), 599–604, 1994.

Chew, W. C., J. M. Jin, and E. Michielssen, Complex coordinate system as a generalized absorbing boundary condition, in *Proceedings of the 13th Annual Review of Progress in Applied Computational Electromagnetics*, pp. 909–914, Appl. Comput. Electromag. Soc., Monterey, Calif., 1997.

Collino, F., and P. Monk, The perfectly matched layer in curvilinear, coordinates, *SIAM J. Sci. Comput.*, *19*(13), 2061–2090, 1998.

Deschamps, G., Electromagnetics and differential forms, *Proc. IEEE*, *69*(6), 676–696, 1981.

Engheta, N., Compact cavity resonators using metamaterials with negative permittivity and permeability, in *Proceedings of ICEAA 2001*, pp. 739–742, Turin, Italy, Univ. of Torino, Italy, 2001.

Fante, R. L., and M. T. McCormack, Reflection properties of the Salisbury screen, *IEEE Trans. Antennas Propagat.*, *36*(10), 1443–1454, 1988.

Garcia-Vidal, F. J., J. M. Pitarke, and J. B. Pendry, Effective medium theory of the optical properties of aligned carbon nanotubes, *Phys. Rev. Lett.*, *78*(22), 4289–4292, 1997.

Gedney, S. D., An anisotropic PML absorbing media for the FDTD simulation of fields in lossy and dispersive media, *Electromagnetics*, *16*, 399–415, 1996.

Hansen, R. C., and M. Burke, Antennas with magneto-dielectrics, *Microwave Opt. Technol. Lett.*, *26*(2), 75–78, 2000.

Hashimoto, O., and O. Mizokami, A method for designing wave absorbers for cylindrical objects, *IEEE Trans. Antennas Propagat.*, *39*(6), 854–857, 1991.

He, J. Q., and Q. H. Liu, A nonuniform cylindrical FDTD algorithm with improved PML and Quasi-PML absorbing boundary conditions, *IEEE Trans. Geosci. Remote Sens.*, *37*(2), 1066–1072, 1999.

Hwang, K.-P., and J.-M. Jin, Application of a hyperbolic grid generation technique to a conformal PML implementation, *IEEE Microw. Guided Wave Lett.*, *9*(4), 137–139, 1999.

Jaggard, D. L., and N. Engheta, Chirosorb as an invisible medium, *Electron. Lett.*, *25*(3), 173–174, 1989.

Jaggard, D. L., N. Engheta, and J. Liu, Chiroshield: A Salisbury/Dallenbach shield alternative, *Electron. Lett.*, *26*(17), 1332–1334, 1990.

Katz, D. S., E. T. Thiele, and A. Taflove, Validation and extension to three dimensions of the Berenger PML absorbing boundary condition, *IEEE Microw. Guided Wave Lett.*, *4*(8), 268–270, 1994.

Kyriazidou, C. A., H. F. Contapagos, and N. G. Alexopoulos, Monolithic waveguide filters using printed photonic-band-

gap materials, *IEEE Trans. Microwave Theory Tech.*, *49*(2), 297–307, 2001.

Landau, L. D., and E. M. Lifshitz, *Statistical Physics, Part 1*, Butterworth-Heinmann, Woburn, Mass., 1980.

Landau, L. D., E. M. Lifshitz, and L. P. Pitaevskii, *Electrodynamics of Continuous Media*, Pergamon, New York, 1984.

Lindell, I. V., S. A. Tretyakov, K. I. Nikoskinen, and S. Ilvonen, BW media-media with negative parameters, capable of supporting backward waves, *Microwave Opt. Technol. Lett.*, *31*(2), 129–133, 2001.

Liu, Q. H., and J. Q. He, Quasi-PML for waves in cylindrical coordinates, *Microwave Opt. Technol. Lett.*, *19*(2), 107–111, 1998.

Maloney, J., M. Kesler, and G. Smith, Generalization of PML to cylindrical geometries, in *Proceedings of the 13th Annual Rev. Prog. Appl. Comp. Eletromag.*, pp. 900–908, Monterey, Calif., 1997.

Norgren, M., Optimal design using stratified bianisotropic media: Application to anti-reflection coatings, *J. Electromagn. Waves Appl.*, *12*, 939–959, 1998.

Norgren, M., and S. He, On the possibility of reflectionless coating of homogeneous bianisotropic layer on a perfect conductor, *Electromagnetics*, *17*, 295–307, 1997.

Pendry, J. B., Negative refraction makes a perfect lens, *Phys. Rev. Lett.*, *85*(18), 3966–3969, 2000.

Pendry, J. B., A. J. Holden, D. J. Robbins, and W. J. Stewart, Low frequency plasmons in thin-wire structures, *J. Phys. Condens. Matter*, *10*, 4785–4809, 1998.

Rozanov, K. N., Ultimate thickness to bandwidth ratio of radar absorbers, *IEEE Trans. Antennas Propagat.*, *48*(8), 1230–1234, 2000.

Sacks, Z. S., D. M. Kingsland, R. Lee, and J.-F. Lee, A perfectly matched anisotropic absorber for use as an absorbing boundary condition, *IEEE Trans. Antennas Propagat.*, *43*(12), 1460–1463, 1995.

Sengupta, L., and M. S. Klushens, *Multilayered Ferroelectric Composite Waveguides*, Army Res. Lab. and Naval Res. Lab., U.S. Patent 5,830,591, Washington D. C., 1998.

Shieh, B., K. C. Saraswat, J. P. McVittie, S. List, S. Nag, M. Islamraja, and R. H. Havemann, Air-gap formation during IMD deposition to lower interconnect capacitance, *IEEE Trans. Electron Devices*, *19*(1), 16–18, 1998.

Sievenpiper, D. F., M. E. Sickmiller, and E. Yablonovitch, 3D wire mesh photonic crystals, *Phys. Rev. Lett.*, *76*, 2480–2483, 1996.

Simovski, C. R., M. Kondratiev, and S. He, An explicit method for calculating the reflection from an anti-reflection structure involving array of c-shaped wire elements, *J. Electromagn. Waves Appl.*, *14*, 1335–1352, 2000.

Slepyan, G. Y., S. A. Maksimenko, A. Lakhtakia, O. M. Yevtsushenko, and A. V. Gusakov, Electronic and electromagnetic properties of nanotubes, *Phys. Rev. B*, *57*, 9485–9497, 1998.

Smith, D. R., W. J. Padilla, D. C. Vier, S. C. Nemat-Nasser, and S. Schultz, Composite medium with simultaneously negative permeability and permittivity, *Phys. Rev. Lett.*, *84*(18), 4184–4187, 2000.

Smith, D. R., D. C. Vier, N. Kroll, and S. Schultz, Microwave transmission through a two-dimensional, isotropic, left-handed metamaterial, *Appl. Phys. Lett.*, *78*(4), 489–491, 2001.

Teixeira, F. L., and W. C. Chew, PML-FDTD in cylindrical and spherical grids, *IEEE Microw. Guided Wave Lett.*, *7*(9), 285–287, 1997.

Teixeira, F. L., and W. C. Chew, Analytical derivation of a conformal perfectly matched absorber for electromagnetic waves, *Microwave Opt. Technol. Lett.*, *17*, 231–236, 1998.

Teixeira, F. L., and W. C. Chew, Differential forms, metrics, and the reflectionless absorption of electromagnetic waves, *J. Electromagn. Waves Appl.*, *13*, 665–686, 1999a.

Teixeira, F. L., and W. C. Chew, Lattice electromagnetic theory for a topological viewpoint, *J. Math. Phys.*, *40*(1), 169–187, 1999b.

Teixeira, F. L., and W. C. Chew, On causality and dynamic stability of perfectly matched layers for FDTD simulations, *IEEE Trans. Microwave Theory Tech.*, *47*(6), 775–785, 1999c.

Teixeira, F. L., K. P. Hwang, W. C. Chew, and J. M. Jin, Conformal PML-FDTD for electromagnetic field simulations: A dynamic stability study, *IEEE Trans. Antennas Propagat.*, *49*(6), 902–907, 2001.

Tretyakov, S. A., Uniaxial omega medium as a physically realizable alternative for the perfectly matched layer (PML), *J. Electromagn. Waves Appl.*, *12*, 821–837, 1998.

Tretyakov, S. A., The perfectly matched layer as a synthetic material with active inclusions, *Electromagnetics*, *20*, 155–166, 2000.

Tretyakov, S. A., Meta-materials with wideband negative permittivity and permeability, *Microwave Opt. Technol. Lett.*, *31*(3), 163–165, 2001.

Venugopal, V. C., A. Lakhtakia, R. Messier, and J.-P. Kucera, Low-permittivity nanocomposite materials using sculptured thin film technology, *J. Vac. Sci. Technol. B*, *18*(1), 32–36, 2000.

Veselago, V. G., Properties of materials having simultaneously negative values of the dielectric (ϵ) and the magnetic (μ) susceptibilities, *Sov. Phys. Solid State*, *8*(12), 2854–2856, 1967.

Walser, R. W., W. Win, and P. M. Valanju, Shape-optimized ferromagnetic particles with maximum theoretical microwave susceptibility, *IEEE Trans. Magn.*, *34*(4), 1390–1392, 1998.

Yablonovitch, E., Photonic band-gap crystals, *J. Phys. Condens. Matter*, *5*(16), 2443–2460, 1993.

Ziolkowski, R. W., The design of Maxwellian absorbers for numerical boundary conditions and for practical applications using artificial engineered materials, *IEEE Trans. Antennas Propagat.*, *45*, 656–671, 1997a.

Ziolkowski, R. W., Time-derivative Lorentz materials and their utilization as electromagnetic absorbers, *Phys. Rev. E*, *55*(6), 7696–7703, 1997b.

Ziolkowski, R. W., Negative permittivity and permeability meta-materials and their applications, in *2001 URSI North American Radio Science Meeting Digest*, p. 382, Boston, Mass., 2001.

Ziolkowski, R. W., and F. Auzanneau, The analysis and design of Maxwellian smart skins, in *1997 URSI North American Radio Science Meeting Digest*, p. 139, Montreal, Canada, 1997.

F. L. Teixeira, ElectroScience Laboratory and Department of Electrical Engineering, Ohio State University, 1320 Kinnear Road, Columbus, OH 43212, USA. (teixeira@ee.eng.ohio-state.edu)